TÜBİTAK

Turkish Journal of Biology

http://journals.tubitak.gov.tr/biology/

Research Article

Turk J Biol
(2017) 41: 378-387
© TÜBİTAK
doi:10.3906/biy-1607-9

FRET-based characterization of K264A, D345A, and Y335A mutants in the human dopamine transporter

Oya ORUN*, Pınar MEGA TİBER
Department of Biophysics, School of Medicine, Marmara University, İstanbul, Turkey

Received: 06.07.2016 • **Accepted/Published Online:** 28.11.2016 • **Final Version:** 20.04.2017

Abstract: The dopamine transporter (DAT) plays a role in the termination of dopaminergic neurotransmission; thereby it is accepted as the primary target of various psychostimulants. N-terminal phosphorylation of DAT has been proposed as a regulator in different DAT functions, such as amphetamine-induced efflux or PKC/PKA-mediated responses. To understand the role of N-terminal conformational changes in dopamine transporter structure and function, the fluorescence resonance energy transfer (FRET) method was applied to various DAT constructs fluorescently labeled at the N-terminus and substrate-induced conformational changes were determined using rhodamine-labeled cocaine analog JHC1-64 in three DAT mutants. The results indicated that the construct with YFP inserted into the N-terminal position-55 displayed effective interaction with the substrate and simultaneous mutation of two serine residues (S7 and S12) to alanine or aspartic acid demonstrated similar phenotypes as their wild-type (WT) counterparts. FRET was detectable for N-terminal p55 YFP WT, Ser/Ala, and Ser/Asp forms, but there was no significant difference among the three mutants, contrary to our expectations based on the previously proposed roles of these serine residues. In addition, three mutants (K264A, D345A, and Y335A) implemented in the position-55 YFP background were also investigated and the importance of Y335 in the translocation cycle and in the process of substrate release was verified.

Key words: Dopamine transporter, fluorescence resonance energy transfer, structure, phosphorylation, N-terminus of DAT

1. Introduction

Dopaminergic signaling has an indispensable role in neurological disorders such as schizophrenia, bipolar disorder, and attention deficit disorder. Duration of dopaminergic signaling, and therefore its regulation, is tightly coupled to the dopamine transporter (DAT), which mediates rapid uptake of dopamine (DA) from the synaptic cleft (Amara and Kuhar, 1993).

The transporter belongs to the family of neurotransmitter transporters also known as sodium symporters (NSSs). These proteins form a large family encompassing other neurotransmitter transporters for norepinephrine, serotonin, glycine, and GABA. All these transporters have the common property of utilizing the energy of the Na^+ gradient to carry the substrate uphill (Rudnick, 1997). In addition to dopamine transport, DAT can also bind several psychostimulant drugs, including amphetamine (AMPH) and cocaine. Indeed, DAT may be the primary target for the rewarding properties of these widely abused psychostimulants.

The N-terminus of transporters has indispensable roles in monoamine transporters' functions. The N-terminus is the primary target of various kinases such as protein kinase A (PKA), protein kinase C (PKC), and Ca^{2+}/calmodulin-dependent kinase (CaM kinase II); however, the role of phosphorylation by these kinases is speculative. The first N-terminal 22 amino acids have previously been shown to be phosphorylated by PKC (Granas et al., 2003). When these 22 amino acids were removed from the N-terminal, DAT (del 22 DAT) phosphorylation was abolished without affecting PKC-induced internalization. In HEK-293 cells stably expressing del-22 DAT, AMPH-induced DA efflux, but not DA uptake, was substantially reduced. Phosphorylation of two serine residues at the N-terminus, Ser 7 and Ser 12, was mainly found to be essential for this response (Khoshbouei et al., 2004; Kahlig et al., 2005). Mutation of serine 7, a site for PKC-mediated phosphorylation, strongly reduced cocaine analog affinity and also changed the zinc modulation of cocaine analog 2β-carbomethoxy-3β(4-fluorophenyl) tropane (CFT) binding, with opposite results in Ala and Asp mutations (Moritz et al., 2013). Other protein kinases also seem to affect nearby serine/threonine residues and phosphorylation of these presumably acts as a modulator of conformational equilibria and inhibitor binding.

* Correspondence: oyaorun@yahoo.com

To address the role of the N-terminus and its phosphorylation upon substrate or inhibitor binding, a technique to characterize conformational changes of the N-terminal tail of DAT expressed in HEK-293 cells was established. By applying fluorescence resonance energy transfer (FRET) between donor fluorophore yellow fluorescent protein (YFP) fused into the N-terminal tail and a rhodamine-labeled cocaine analog bound in the transmembrane domain of DAT, the movement of the tail relative to the fixed rhodamine position was monitored. Evaluation of FRET signals revealed close encounters between the residues upstream from position 55 and the substrate binding site. DA uptake and binding of 2β-carbomethoxy-3β-(4-iodophenyl) tropane (RTI-55) were unaffected upon phosphorylation.

N-terminal changes invoked by inhibitor binding were further investigated in mutants that have been shown to have roles in Zn^{2+}-induced activity changes. Zn^{2+} binds to a high-affinity Zn^{2+} binding site in DAT, shaped by three coordinating residues: His 193, His 375, and Glu 396. The effect of Zn^{2+}, which was shown to be a potent noncompetitive inhibitor of dopamine uptake, was modulated by different mutations. The transporters carrying one of the three mutations, K264A, Y335A, or D345A , were all characterized by their decreased V_{max} and K_m values for [^{3}H] dopamine uptake and the addition of Zn^{2+} into the medium resulted in a dose-dependent increase in substrate intake (Loland et al., 2004). Physiologic concentrations of Zn^{2+} also affected inhibitor binding and AMPH-induced efflux in DAT (Scholze et al., 2002; Meinild et al., 2004). In the present study, new DAT forms with a YFP tag were constructed, and it was determined that the insertion of a large YFP tag into p55 of DAT did not affect any Zn^{2+}-induced properties of Zn^{2+}-sensitive mutants. Later, structural properties were investigated by FRET analyses and confirmed previously suggested roles of these mutants to alter the distribution between different equilibrium states of DAT transport. In particular, Tyr-335 mutation clearly disrupted energy transfer, providing further evidence for the role of Tyr-335 in an intramolecular "gating network" and conformational equilibrium of the protein.

2. Materials and methods

2.1. Cloning

A synthetic hDAT gene with artificially introduced restriction enzyme sites (SynDAT) was used as a template in site-directed mutagenesis studies (Loland et al., 2004). This gene was inserted into the bicistronic mammalian expression vector pCIHygro and the protein was shown to have identical expression and function to hDAT (Rees et al., 1996; Saunders et al., 2000, Hastrup et al., 2001). The constructs containing YFP were synthesized by two-step PCR using Phusion polymerase (Finnzymes, Espoo, Finland) and SynDAT as a template. All constructs were confirmed by restriction enzyme digestion and by automated DNA sequence analysis (MWG Biotech, Ebersberg, Germany). All restriction enzymes were from New England Biolabs (Beverly, MA, USA).

2.2. Cell culture and transfections

Cell culture and transfection were maintained as described previously (Orun et al., 2009). For stable cell lines, the transfected pool was selected using 350 μg/mL hygromycin (Invitrogen, Carlsbad, CA, USA). Stable cell lines containing K264A, D345A, and Y335A mutations were maintained with a supplement of 10 μM Zn^{2+} in the culture.

2.3. Uptake experiments

Uptake assays were performed using 2,5,6-[^{3}H]-dopamine (7-21 Ci/mmol) (Amersham Biosciences, Little Chalfont, UK). Cells were seeded at a density of 1×10^5 cells/well in 24-well plates coated with 20 mg/mL poly-D-lysine (Sigma, St. Louis, MO, USA) in PBS buffer 2 days before the assay. The uptake buffer contained 10 μM catechol-o-methyltransferase inhibitor Ro 41-0960 to prevent dopamine degradation. Unlabeled dopamine ligands (Research Biochemicals, Billingham, UK) were added in concentrations of 10 nM to 1 mM. After addition of radioactive dopamine (90 nM [^{3}H] dopamine), the uptake reaction was performed in 5 min at 37 °C. All samples were analyzed in triplicate. Statistically analyzed assays are the result of at least three independent experiments, since this was found to be sufficient for ligand binding and activity tests (Loland et al., 2002). The samples were counted in a Wallac Tri-Lux β-scintillation counter (NEN). Data were analyzed by nonlinear regression analysis using Graph Prism v5.01 fitting and plotting software (GraphPad, San Diego, CA, USA).

2.4. Donor bleach FRET

Cells were seeded in 8-well Lab-Tek chambers at 4×10^4 cells/well 2 days before the experiment. The donor bleach method was applied, in which protection of YFP from bleaching (488 nm, 60% laser power) was an indicator of FRET between the donor YFP and the acceptor rhodamine-labeled cocaine analog (JHC1-64). A wavelength of 488 nm at 10% power was used as excitatory light, while the emission spectrum was confined using a BP 505-530 filter. A 4× zoom was applied during all measurements. RTI-55 was used as a control nonfluorescent cocaine analog. Cells were bleached in the YFP channel by scanning a region of interest (ROI) 60 times using the 514 argon laser line. The number of repeats was 8–12 for each experiment, with various ROI selections from different cells. Bleaching time constants (t_{bl}) of donor-only (t_d) or donor- and acceptor ($t_{d,a}$)-labeled cells were calculated for each image and energy transfer efficiencies were calculated using E(%) =

$100 \times [1 - (\square_d / \square_{d,a})]$ (Damjanovich et al., 1995). Distances were determined using efficiency values according to the following formula: $r = R_0 \{(1 / E - 1)\}^{1/6}$.

3. Results

3.1. Characterization of phospho-mimicking mutants in the p55 YFP background

YFP was introduced into position 55 and phospho-mimicking mutants serine-to-alanine (Ser7/12Ala) or serine-to-aspartic acid (Ser7/12Asp) were constructed as shown in Figure 1. Transient or stable cell lines transfected with constructs were then tested for their dopamine uptake ability, surface expression, and FRET.

Previous studies reported that truncation of the first 58 amino acids of DAT (del 58 DAT) changed neither localization nor surface expression and uptake, but truncation of the first 65 amino acids abolished dopamine transport, indicating a crucial role for residues between 59 and 65 (Gu et al., 2001; Sorkina et al., 2003). In addition, mutation of Thr 62 showed a clear influence on the influx–efflux balance of the transporter, and a salt bridge between Arg60 and Asp436 was shown to drive DAT to an outward-facing substrate binding conformation (Kniazeff et al., 2008; Guptaroy et al., 2009). Therefore, YFP, a 27-kDa tag, was introduced into position 55, a few residues preceding these crucial amino acids, and surface expression of the construct was examined. Surface localization of this construct, together with other mutants built in this study, was found to be comparable to wild-type (WT) human SynDAT (Figures 2A–2C).

Following the construction of N-term p55 YFP, double-Ser mutants (mutated either to aspartic acid [Ser7Asp and Ser12Asp] to mimic the phosphorylated state of the transporter or to alanine to eliminate phosphorylation [Ser7Ala and Ser12Ala] on the N-term p55 YFP background) were established, and dopamine uptake capabilities were determined for all constructs (Figure 3A).The EC_{50} values for all constructs were similar, as summarized in Table 1. The values are from means of three independent experiments performed in triplicate.

Affinities for cocaine analog RTI-55 were also determined for all groups. Competition binding

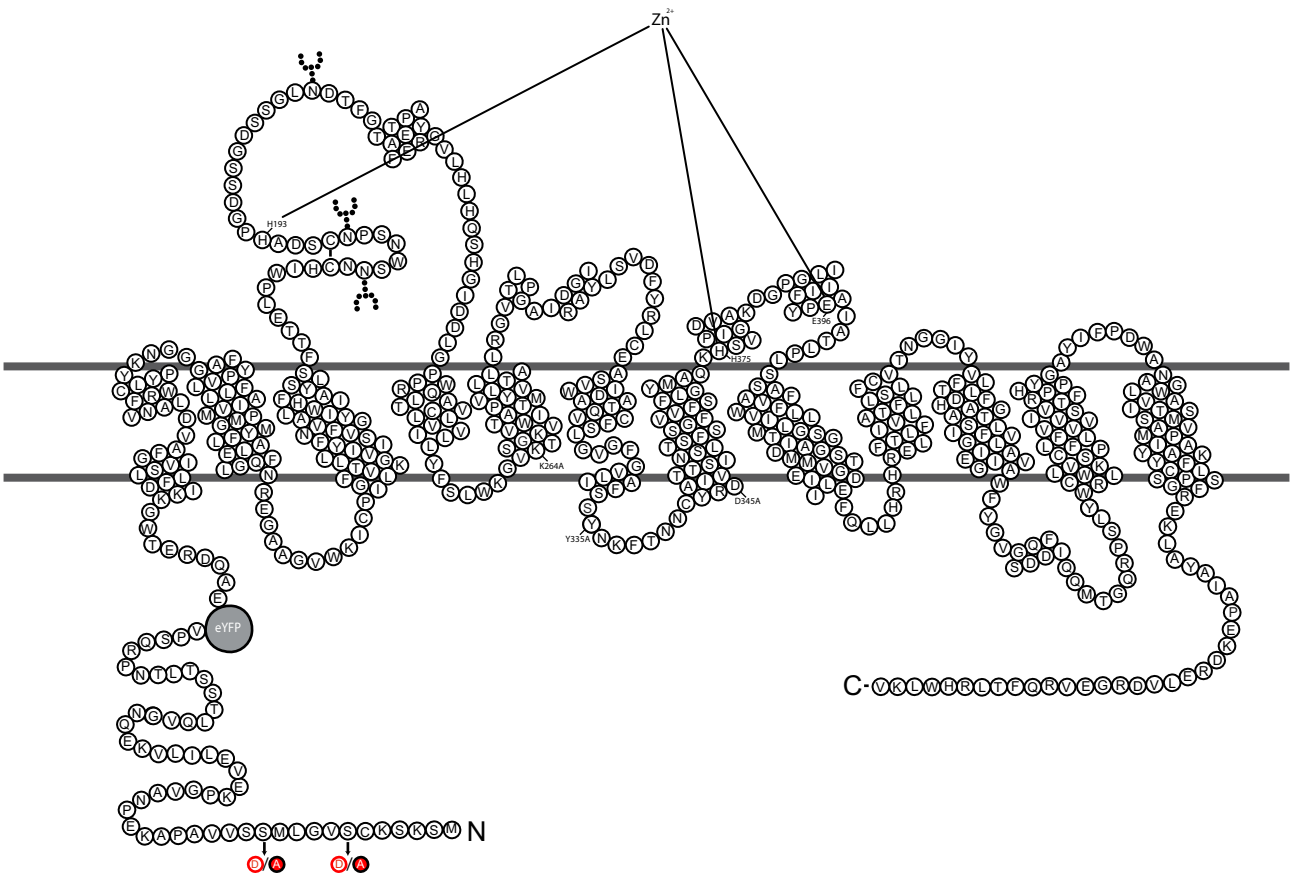

Figure 1. Topologic representation of human SynDAT with introduced mutations. Ser/Ala (Ser7/12 Ala) and Ser/Asp (Ser7/12 Asp) mutations (pink/red dots) together with K264A, D345A, and Y335A mutations on the N-term p55 YFP background depicted in the same picture.

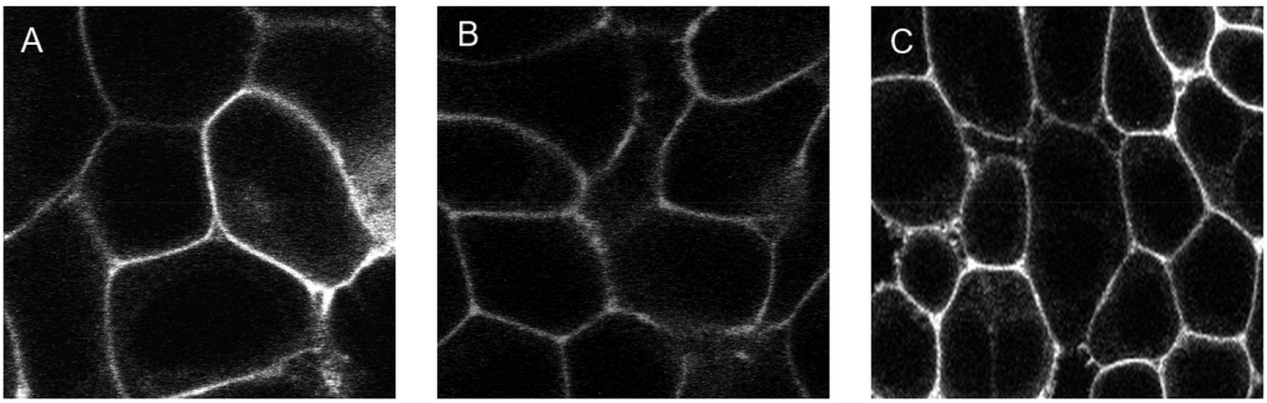

Figure 2. Representative picture for surface expression of constructs: (A) WT, (B) Ser/Asp (S7D and S12D) mutant, and (C) Y335A mutant forms of N-term p55 YFP human SynDAT. Cells were seeded into 8-well Lab-Tek II glass chamber slides (Nalge, Penfield, NY, USA) 24 h before analysis and visualized using a Zeiss (Oberkochen, Germany) LSM 510 confocal laser scanning microscope with an oil immersion 63× water objective. A 150-mW Ar-Kr laser was used for the excitation of YFP at 488 nm, and the emitted light passed through a 505-nm long-pass filter.

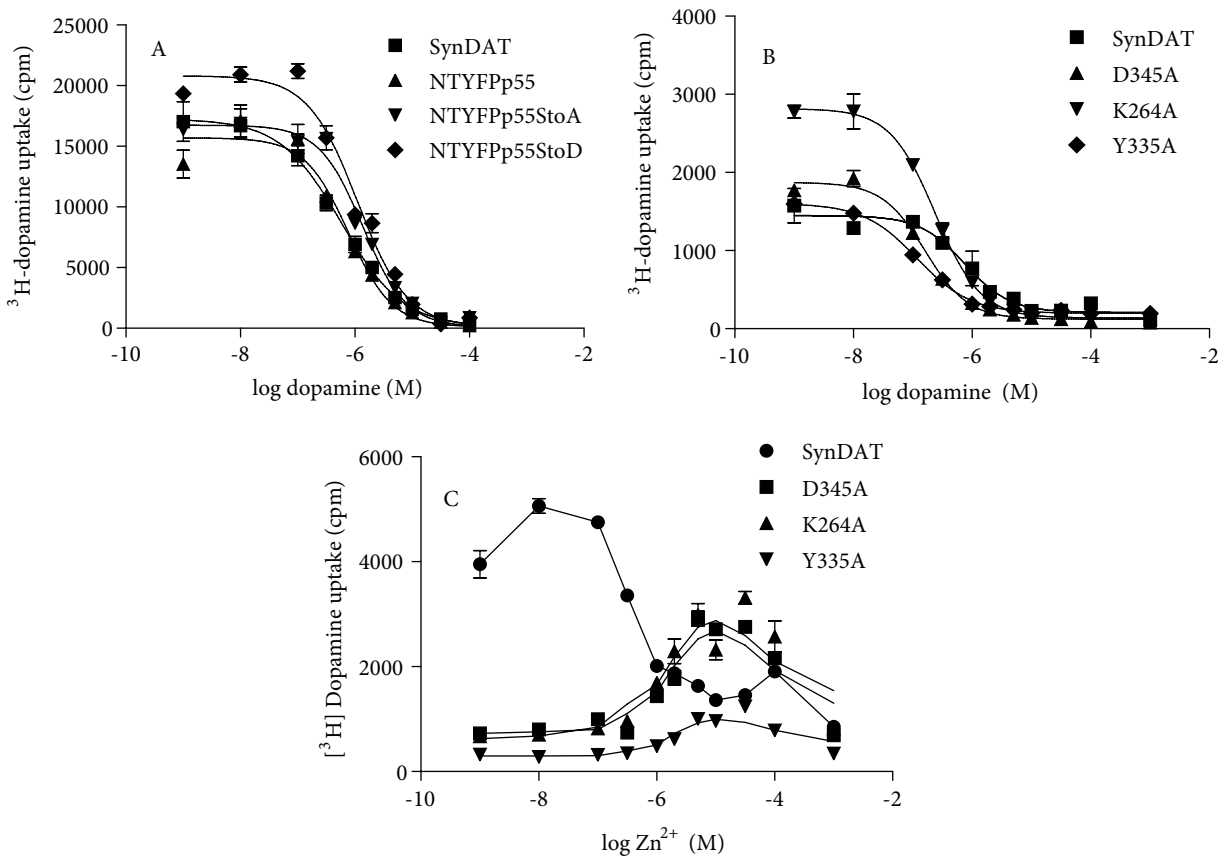

Figure 3. [^{3}H] dopamine uptake of N-term p55 YFP-labeled DAT mutants. YFP was placed at position 55 of the dopamine transporter by two-step PCR-based mutagenesis in the background of the SynDAT template, as described in the text. The effect of phosphorylations at two serine positions (Ser7 and Ser12), together with zinc-activating mutations, was examined. (A) Uptake curves of N-term p55 YFP-labeled WT human SynDAT, Ser/Ala, and Ser/Asp mutants with increasing concentrations of dopamine. (B) Uptake curves of N-term p55 YFP-labeled WT human SynDAT and K264A, D345A, and Y335A mutants with increasing concentrations of dopamine. (C) Uptake curves of N-term p55 YFP-labeled WT human SynDAT and K264A, D345A, and Y335A mutants with zinc addition. All experiments were performed at least in triplicate.

Table 1. [^{3}H] dopamine uptake and binding characteristics of human SynDAT and its YFP-labeled mutants.

	EC_{50} (μM)	V_{max}	K_m (μM)
	[SE interval]	(fmol/min/10^5 cells ± SE)	[SE interval]
SynDAT	1.45 [1.01–2.08]	20,673 ± 2676	1.45 [1.01–2.08]
NTp55YFPSynDAT	0.92 [0.76–1.11]	17,327 ± 4269	1.15 [0.94–1.41]
NTp55YFPSynDAT StoA	1.0 [0.88–1.15]	14,482 ± 1212	0.95 [0.83–1.08]
NTp55YFPSynDAT StoD	1.13 [1.12–1.14]	17,074 ± 1827	1.06 [1.04–1.08]

The values were calculated from nonlinear regression analysis of uptake data using GraphPad Prism v5.0. All values were calculated from the means of at least three repetitions.

experiments were performed on HEK-293 cells expressing the appropriate constructs and IC_{50} values for cocaine analog RTI-55 were 5.85 nM (4.45–7.7) for WT human SynDAT, 2.52 nM (1.65–3.85) for N-term p55 YFP SynDAT, 3.07 nM (1.67–5.67) for N-term p55 YFP SynDAT/S-to-A, and 3.43 nM (2.42–4.86) for N-term p55 YFP SynDAT/S-to-D constructs.

3.2. Characterization of mutant Zn^{2+}-responsive residues in the p55 YFP background

All three Zn^{2+}-responsive constructs built in this study, namely N-term p55 YFP D345A, N-term p55 YFP K264A, and N-term p55 YFP Y335A, displayed reduced V_{max} and K_m values compared to the WT in dopamine uptake assays (Table 2). V_{max} for N-term p55 YFP D345A and K264A was nearly 10% of N-term p55 YFP WT human SynDAT, while it further decreased to 6% in the N-term p55 YFP Y335A construct (Figure 3B).

The effect of Zn^{2+} on uptake was also similar to the previously reported behavior of WT hDAT and its Zn^{2+}-responsive mutants (Loland et al., 2003). Zn^{2+} showed biphasic inhibition of N-term p55 YFP-tagged human SynDAT (data not shown) and that inhibition was converted to stimulation in the aforementioned N-term p55 YFP-tagged mutants in a dose-dependent manner (Figure 3C).

These results confirmed that placing a YFP tag into position 55 did not cause a significant change in the functionality of the WT or mutant forms of the transporter, neither in dopamine uptake nor in the potentiating effect of Zn^{2+}.

3.3. FRET analyses

FRET was examined between a rhodamine-labeled cocaine analog (JHC1-64) and N-term p55 YFP human SynDAT mutants. The ligand was found in FRET distance

Table 2. [^{3}H] dopamine uptake and binding characteristics of human SynDAT and its Zn^{2+}-sensitive mutants.

	EC_{50}(μM) [SE interval]	V_{max} (fmol/min/10^5 cells ± SE)	K_m (μM) [SE interval]	IC_{50} (μM) (Zn^{2+})	K_i (RTI-55)
NTp55YFP SynDAT	0.92 [0.76–1.11]	13,842 ± 3413	1.15 [0.94–1.41]	0.47	5.5 [4.9–6.2]
NTp55YFP SynDATK264A	1.37 [1.36–1.38]	1697 ± 132	0.68 [0.66–0.69]	1.98	16.3 [13.4–2.00]
NTp55YFP SynDATD345A	0.8 [0.7–0.8]	1591 ± 545	0.95 [0.47–1.9]	2.06	5.5 [4.9–6.2]
NTp55YFP SynDATY335A	0.14 [0.13–0.14]	895 ± 59	0.29 [0.18–0.48]	3.9	300 [217–439]

The values were calculated from nonlinear regression analysis of uptake data using GraphPad Prism v5.0. Zn^{2+} inhibition of [^{3}H] dopamine uptake was fitted to either a two-site or a one-site model. The binding of RTI-55, a nonfluorescent cocaine analog control used in FRET measurements, was also tested in mutant constructs. All values were calculated from the means of at least three repetitions.

with the YFP label in N-term p55 YFP human SynDAT, and there was no detectable change in FRET when S/D or S/A mutations were introduced (Figures 4A and 4B).

FRET was also applied to mutants that have Zn^{2+}-induced effects on both substrate- and inhibitor-binding properties of WT DAT (Figures 5A–5C). Prolongation of half-life was observed in N-term p55 YFP K264A, but the FRET signal was weak with a calculated proximity of 63 Å between position 55 and the bound cocaine analog, the same as for the S/D form. In the D345A mutation, fluorescent pairs were still in FRET distance, but the proximity was lower (Table 3). There was no detectable energy transfer in the Y335A form. Affinity of the Y335A construct for cocaine analog RTI-55 was also very low. These findings are pertinent to the dramatic changes observed in Y335A mutants, verify N-term R60–Y335 bond formation, and show that N-term YFP-tagged DAT can be a useful tool to study intramolecular conformational regulation.

4. Discussion

DAT is the major target for psychostimulants like cocaine and amphetamine. The last decade provided important insights into to the structure–function relationship of this large integral protein. Crystallization of a bacterial homolog, leucine transporter (LeuT), and more recently, X-ray models of DAT from *Drosophila* (dDAT) showed that the 3D structure of transporters have high folding similarities, despite their low sequence identity across species (22% for LeuT and 50% for dDAT with the eukaryotic NSS family) (Yamashita et al., 2005; Forrest et

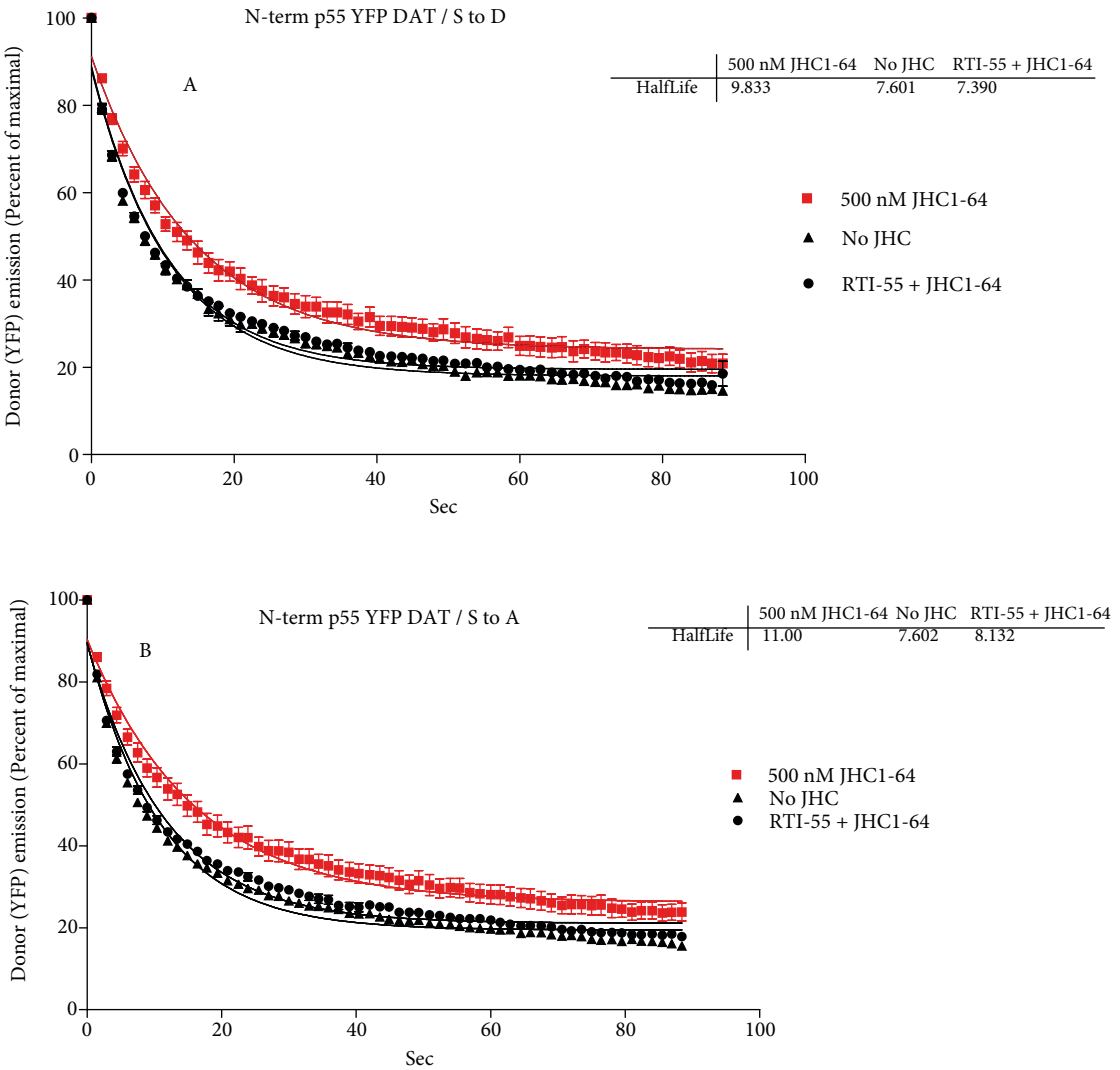

Figure 4. FRET in N-term p55 YFP-labeled (A) S-to-D and (B) S-to-A mutants. Cocaine analog JHC1-64-induced changes in FRET in N-term p55 YFP-labeled S-to-D and S-to-A mutants were reversed by the addition of nonfluorescent cocaine analog RTI-55. Data are means of 8–12 independent experiments.

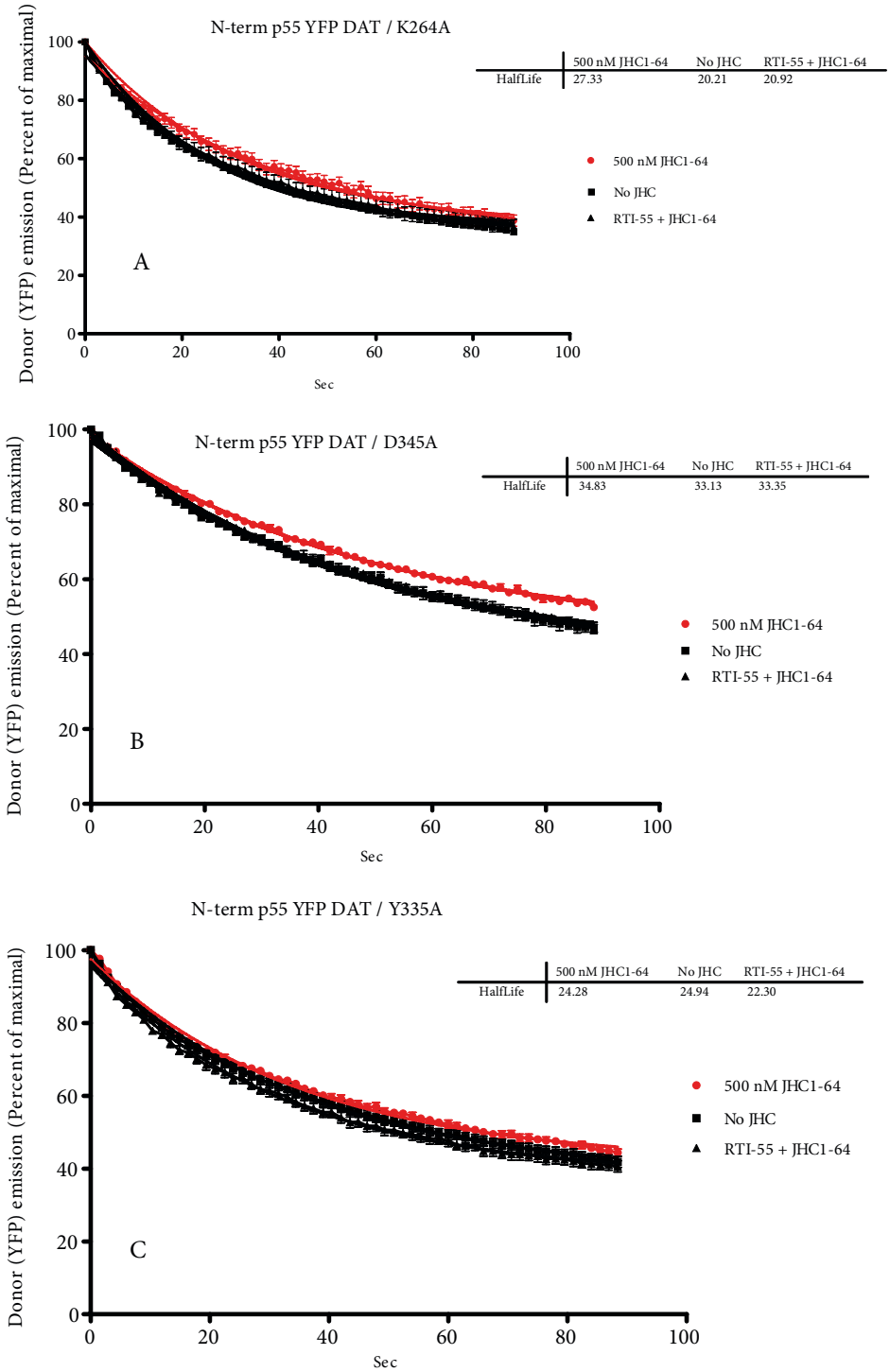

Figure 5. FRET in N-term p55 YFP-labeled (A) K264A, (B) D345A, and (C) Y335A mutants. Calculated half-lives imply FRET proximities in reducing order for K264A, D345A, and Y335A, respectively. Both uptake experiments and FRET studies indicated that position Y335 has a critical role in function, and that mutation of this residue severely impairs conformational stability distribution during substrate translocation. Data are means of 8–12 independent experiments.

Table 3. FRET efficiencies and estimated intramolecular proximities between the rhodamine-labeled cocaine analog and the YFP protein inserted into the N-terminus of human SynDAT.

	E (%)	r (Å)
NTp55YFPSynDAT	14	69.4
NTp55YFPSynDATStoA	31	58.6
NTp55YFPSynDATStoD	23	62.7
NTp55YFPSynDATK264A	20	62.9
NTp55YFPSynDATD345A	0.05	83.7
NTp55YFPSynDATY335A	-	-

Bleaching time constants (t_{bl}) of donor-only (t_d) or donor- and acceptor ($t_{d,a}$)-labeled cells were calculated using GraphPad one-phase exponential decay analysis. Energy transfer efficiencies and distances were calculated as described in Section 2. R_0 was estimated as 51.29 Å for a YFP–rhodamine pair using available values for the quantum yield and extinction coefficients of the donor–acceptor pair.

al., 2007; Indarte et al., 2007; Beuming et al., 2008; Shan et al., 2011; Krishnamurthy and Gouaux, 2012; Penmatsa et al., 2013). These studies, together with models built upon the available data, indicated that the binding sites for cocaine and cocaine analogs are deeply buried between TM 1, 3, 6, and 8 and overlap with binding sites for substrates such as dopamine and amphetamine (Beuming et al., 2008).

Amphetamine is a dopamine reuptake inhibitor. Besides its role as a blocker of DA uptake, the main effect of amphetamine is through induction of DA efflux. This process works by increasing the number of inward-facing binding sites. Phosphorylation of serine residues (Ser7 and Ser12) in the N-terminal tail of DAT regulates amphetamine-induced DA efflux through an unknown mechanism (Khoshbouei et al., 2004). To characterize conformational changes upon phosphorylation of N-terminus, FRET distances between the N-terminus involving phospho-mimicking mutations and the cocaine-binding site were assessed. Since the crystal structure data of LeuT start from position 56 of wild-type DAT, a YFP tag was placed into position 55. These results, in accordance with the model based on the crystal structure of LeuT, verify the role of residues upstream to position 55 in activation of DAT (Beuming et al., 2008). In an earlier study, we reported that there is no FRET interaction between the extreme N-terminus or its phospho-mimicking mutants and the cocaine-analog binding site (Orun and Tiber, 2015). The lack of FRET for the N-term position 1, together with the current finding for position 55, suggests that the very end of DAT has an extended structure, further away from ligand binding sites.

Since preliminary experiments designed to determine binding and interaction domains of DAT relied on manipulating an endogenous Zn^{2+} binding site, we also wanted to explore possible large-scale conformational changes in cocaine-analog binding in the presence of Zn^{2+}. Zn^{2+}, in micromolar concentrations, has been shown to act as a potent noncompetitive blocker of dopamine uptake and to stabilize the outward-facing conformation of DAT. Zn^{2+} also potentiates binding of cocaine-like blockers, such as WIN 35,428. Identification of Zn^{2+} binding sites His193, His375, and Glu396 pointed to a spatial proximity between the EC2 loop and the top of the TM7 and TM8 domains. Recently, D206 was confirmed as the fourth coordinating residue in zinc binding (Stockner et al., 2013). The mutation of an intracellular tyrosine to alanine (Y335A) converted the inhibitory Zn^{2+} switch into an activating one. This tyrosine was placed in a conserved trafficking motif (YXXF) and mutation of this residue did not change the surface expression or internalization pattern of the transporter. The Y335A mutant had greatly reduced dopamine reuptake compared to other constructs, and uptake velocity was less than 1% of that of the wild type. V_{max}, however, was found to be partially restored when Zn^{2+} was added in micromolar concentrations, indicating that Tyr-335 may be critical in the partitioning of conformational states in the translocation cycle of DAT (Loland et al., 2002). Additionally, there was a 20-fold increase in affinity for substrates, contrary to a 150-fold decrease for inhibitors such as CFT or RTI-55 (Loland et al., 2004). Substitution experiments showed that K264A, D345A, and D436A mutants also produced a phenotype similar to Y335A.

To better understand the conformational changes in DAT after binding to inhibitors, the efficiency of fluorescence energy transfer in N-terminally labeled p55 YFP mutants containing one of the mutations Y335A, D345A, or K264A was measured. Dopamine uptake capacities of all mutants were tested and found to be reduced in all constructs, as expected. In N-term p55 YFP-tagged K264A human SynDAT, JHC1-64 was in FRET distance with respect to position 55. The distance was greater than 80 Å for N-terminus p55 YFP-tagged D345A and was out of FRET range (>100 Å) for the N-terminus p55 YFP-tagged Y335A mutant.

The relationship between the N-terminus and substrate binding site is of critical importance in DAT function. In recent years, two substrate binding sites, namely S1- and S2-, were well clarified by modeling and molecular dynamic studies as well as experimental data (Shan et al., 2011; Cheng et al., 2015; Zomot et al., 2015). Molecular details of the communication and allosteric interaction between the two sites and the proposed mechanism in substrate release seem to involve many residues and various dynamics. According to these studies, DA release from the S1 site involves a sequence of arrangements involving F69, F76, F332, W63, and Y335. The role of the N-terminus as a network defining an intracellular "gate" was also assessed by a proposed salt bridge between R60 and D436, which is stabilized by a cation–p interaction between R60 and Y335 (Kniazeff et al., 2008). Furthermore, Guptaroy et al. showed that T62 mutation in the N-terminus results in dramatically reduced [^{3}H] dopamine uptake and this mutant prefers an inward-facing conformation, similar to Y335A mutants (Guptaroy et al., 2009). D345, on the other hand, was characterized as an important element in both forward and reverse transport of DA. Although uptake inhibition by inhibitors did not seem to be seriously affected by D345 mutants, all D345 mutants had extremely low V_{max} and K_m values for DA uptake (Chen et al., 2004). D345 possibly has a role in inhibitor binding and mutation of that residue converts DAT to a partially active state, which alters the interaction of cocaine analogs with the transporter (Chen et al., 2004). Although available data do not support direct contact between D345 and Y335, both residues have been suggested to be the active participants of a network of intermolecular connections taking place during substrate translocation. The present findings indicate that both mutants result in the diminution of FRET between TM1a and the substrate binding state upon cocaine binding, though the effect on D345 is less dramatic.

Overall, the data presented here emphasize the role of the interaction between parts of the N-terminus 55 amino acids further from the extreme end and other TM regions, especially TM6b, in relation to S1-site occupation and dopamine translocation. No major change in conformation was detected between the phosphorylated and nonphosphorylated forms of the N-terminus upon cocaine analog binding. These findings support the estimated movement of the N-terminus, specifically the movement of region TM1a away from TM6b upon Y335A mutation. They also show that Tyr 335 and Asp 345 are active parts of the conformational rearrangement during the transition from the DA-bound S1 state to the inward-facing conformation, while the role of K264 may be more subsidiary in comparison.

Acknowledgments

We thank Dr Ulrik Gether and Dr Soren GF Rasmussen for their invaluable support through the study and critical reading of the manuscript.

References

Amara SG, Kuhar MJ (1993). Neurotransmitter transporters: recent progress. Annu Rev Neurosci 16: 73-93.

Beuming T, Kniazeff J, Bergmann ML, Shi L, Gracia L, Raniszewska K, Newman AH, Javitch JA, Weinstein H, Gether U et al. (2008). The binding sites for cocaine and dopamine in the dopamine transporter overlap. Nat Neurosci 11: 780-789.

Chen N, Rickey J, Berfield JL, Reith MEA (2004). Aspartate 345 of the dopamine transporter is critical for conformational changes in substrate translocation and cocaine binding. J Biol Chem 279: 5508-5519.

Cheng MH, Block E, Hu F, Cobanoglu MC, Sorkin A, Bahar I (2015). Insights into the modulation of dopamine transporter function by amphetamine, orphenadrine, and cocaine binding. Front Neurol 6: 134.

Damjanovich S, Vereb G, Schaper A, Jenei A, Matkó J, Pascual Starink JP, Fox GQ, Arndt-Jovin DJ, Jovin TM (1995). Structural hierarchy in the clustering of HLA class I molecules in the plasma membrane of human lymphoblastoid cells. P Natl Acad Sci USA 92: 1122-1126.

Forrest LR, Tavoulari S, Zhang YW, Rudnick G, Honig B (2007). Identification of a chloride ion binding site in Na+/Cl -dependent transporters. P Natl Acad Sci USA 104: 12761-12766.

Granas C, Ferrer J, Loland CJ, Javitch JA, Gether U (2003). N-terminal truncation of the dopamine transporter abolishes phorbol ester- and substance p receptor-stimulated phosphorylation without impairing transporter internalization. J Biol Chem 278: 4990-5000.

Gu HH, Wu X, Giros B, Caron MG, Caplan MJ, Rudnick G (2001). The NH_2-terminus of norepinephrine transporter contains a basolateral localization signal for epithelial cells. Mol Biol Cell 12: 3797-3807.

Guptaroy B, Zhang M, Bowton E, Binda F, Shi L, Weinstein H, Galli A, Javitch JA, Neubig RR, Gnegy ME (2009). A juxtamembrane mutation in the n terminus of the dopamine transporter induces preference for an inward-facing conformation. Mol Pharmacol 75: 514-524.

Hastrup H, Karlin A, Javitch JA (2001). Symmetrical dimer of the human dopamine transporter revealed by cross-linking Cys-306 at the extracellular end of the sixth transmembrane segment. P Natl Acad Sci USA 98: 10055-10060.

Indarte M, Madura JD, Surratt CK (2007). Dopamine transporter comparative molecular modeling and binding site prediction using the LeuTAa leucine transporter as a template. Proteins Struct Funct Bioinforma 70: 1033-1046.

Kahlig KM, Binda F, Khoshbouei H, Blakely RD, McMahon DG, Javitch JA, Galli A (2005). Amphetamine induces dopamine efflux through a dopamine transporter channel. P Natl Acad Sci USA 102: 3495-3500.

Khoshbouei H, Sen N, Guptaroy B, Johnson L, Lund D, Gnegy ME, Galli A, Javitch JA (2004). N-terminal phosphorylation of the dopamine transporter is required for amphetamine-induced efflux. PLoS Biol 2: e78.

Kniazeff J, Shi L, Loland CJ, Javitch JA, Weinstein H, Gether U (2008). An intracellular interaction network regulates conformational transitions in the dopamine transporter. J Biol Chem 283: 17691-17701.

Krishnamurthy H, Gouaux E (2012). X-ray structures of LeuT in substrate-free outward-open and apo inward-open states. Nature 481: 469-474.

Loland CJ, Grånäs C, Javitch JA, Gether U (2004). Identification of intracellular residues in the dopamine transporter critical for regulation of transporter conformation and cocaine binding. J Biol Chem 279: 3228-3238.

Loland CJ, Norgaard-Nielsen K, Gether U (2003). Probing dopamine transporter structure and function by zn2+-site engineering. Eur J Pharmacol 479: 187-197.

Loland CJ, Norregaard L, Litman T, Gether U (2002). Generation of an activating Zn^{2+} switch in the dopamine transporter: mutation of an intracellular tyrosine constitutively alters the conformational equilibrium of the transport cycle. P Natl Acad Sci USA 99: 1683-1688.

Meinild AK, Sitte HH, Gether U (2004). Zinc potentiates an uncoupled anion conductance associated with the dopamine transporter. J Biol Chem 279: 49671-49679.

Moritz AE, Foster JD, Gorentla BK, Mazei-Robison MS, Yang J-W, Sitte HH, Blakely RD, Vaughan RA (2013). Phosphorylation of dopamine transporter serine 7 modulates cocaine analog binding. J Biol Chem 288: 20-32.

Orun O, Rasmussen S, Gether U (2009). Introducing tetraCys motifs at two different sites results in a functional dopamine transporter. Acta Biol Hung 60: 15-25.

Orun O, Tiber PM (2015). Determination of spatial proximity between the N-terminus and cocaine binding site of the dopamine transporter by FRET. Marmara Medical Journal 28: 1-6.

Penmatsa A, Wang KH, Gouaux E (2013). X-ray structure of dopamine transporter elucidates antidepressant mechanism. Nature 503: 85-90.

Rees S, Coote J, Stables J, Goodson S, Harris S, Lee MG (1996). Bicistronic vector for the creation of stable mammalian cell lines that predisposes all antibiotic-resistant cells to express recombinant protein. Biotechniques 20: 102-110.

Rudnick G (1997). Neurotransmitter Transporters: Structure, Function and, Regulation. New York, NY, USA: Springer Science & Business Media.

Saunders C, Ferrer JV, Shi L, Chen J, Merrill G, Lamb ME, Leeb-Lundberg LM, Carvelli L, Javitch JA, Galli A (2000). Amphetamine-induced loss of human dopamine transporter activity: an internalization-dependent and cocaine-sensitive mechanism. P Natl Acad Sci USA 97: 6850-6855.

Scholze P, Nørregaard L, Singer EA, Freissmuth M, Gether U, Sitte HH (2002). The role of zinc ions in reverse transport mediated by monoamine transporters. J Biol Chem 277: 21505-21513.

Shan J, Javitch JA, Shi L, Weinstein H (2011). The substrate-driven transition to an inward-facing conformation in the functional mechanism of the dopamine transporter. PLoS One 6: e16350.

Sorkina T, Doolen S, Galperin E, Zahniser NR, Sorkin A (2003). Oligomerization of dopamine transporters visualized in living cells by fluorescence resonance energy transfer microscopy. J Biol Chem 278: 28274-28283.

Stockner T, Montgomery TR, Kudlacek O, Weissensteiner R, Ecker GF, Freissmuth M, Sitte HH (2013). Mutational analysis of the high-affinity zinc binding site validates a refined human dopamine transporter homology model. PLoS Comput Biol 9: e1002909.

Yamashita A, Singh SK, Kawate T, Jin Y, Gouaux E (2005). Crystal structure of a bacterial homologue of Na^+/Cl^--dependent neurotransmitter transporters. Nature 437: 215-223.

Zomot E, Gur M, Bahar I (2015). Microseconds simulations reveal a new sodium-binding site and the mechanism of sodium-coupled substrate uptake by LeuT. J Biol Chem 290: 544-555.